Radiative cascades from charged semiconductor quantum dots

E. Poem,[1,*] Y. Kodriano,[1] C. Tradonsky,[1] B. D. Gerardot,[2] P. M. Petroff,[2] and D. Gershoni[1]
[1]*Department of Physics, The Technion–Israel Institute of Technology, Haifa 32000, Israel*
[2]*Materials Department, University of California, Santa Barbara, California 93106, USA*
(Received 30 December 2009; published 5 February 2010)

We measured two-photon radiative cascades due to sequential recombination of quantum-dot confined electron-hole pairs in the presence of an additional spectator charge carrier. We use temporally resolved polarization sensitive intensity correlation measurements to fully characterize these radiative cascades. We identified direct, all optical cascades involving spin-blockaded intermediate states, and indirect cascades, in which nonradiative relaxation precedes the second radiative recombination. Our measurements provide spin dephasing rates of confined single carriers.

DOI: 10.1103/PhysRevB.81.085306 PACS number(s): 78.67.Hc, 42.50.Ar, 73.21.La

Sequential emission of two photons (radiative cascade) from excited atoms played an essential role in understanding quantum mechanics in general and entanglement between quantum systems, in particular.[1,2] This quantum correlation between the degrees of freedom of different particles carries with it nonlocal properties which are essential for future technologies such as quantum teleportation, cryptography, and computation.[3–6]

Semiconductor quantum dots (QDs) strongly localize charge carriers, and discretize their energy-level spectrum, in a similar way to electrons in atoms. Their affinity to conventional technology and ease of integration into large structures make them candidates for implementation of the basic building blocks for solid-state-based quantum logic devices.[7] Like electrons in isolated atoms, the spin of confined charge carriers in QDs can be described as a quantum two-level system (qubit). Quantum control over these spins is a significant experimental and theoretical challenge since, as in all solid-state systems, they are inherently less isolated from their environment than isolated atomic systems. Recent reports on successful accomplishments of quantum control over such qubits[8–10] are quite encouraging, particularly since the charge state of QDs are easily controlled externally.

QDs devices have shown to provide deterministic, controllable single-photon sources.[11–15] Radiative cascades in neutral QDs (Refs. 16–19) demonstrated their potential as deterministic sources for polarization-entangled photon pairs.[20,21] The neutral radiative cascade[22,23] leaves the QD empty of charge carriers. This is essential for entangling the emitted photons since otherwise the remaining carrier's spin betrays the required "which path" ambiguity.[24,25] Neutrality prevents, however, the important benefit of correlating between the emitted photons' polarizations (flying qubits) and the local carrier's spins (anchored qubits). The situation is different in charged QDs, where quantum correlations exist between the flying and anchored qubits.

In this paper we report on two-photon radiative cascades in the presence of an additional spectator positive charge carrier. We believe that our observations and the understanding that we gain provide an important link between anchored and flying qubits, thereby marking a significant step toward applying QDs as venues for quantum information processing.

The energy levels of a positively charged QD (Refs. 26 and 27) containing up to three holes (fat arrows) and two electrons (thin arrows) are schematically described in Fig. 1(a). The figure presents also the relevant radiative (solid arrows) and nonradiative (curly arrows) total-spin-conserving transitions between these levels. The two-photon radiative cascades start from the ground level of the three hole and two electron state. This level is mainly composed of the few-carrier configuration where two spin-paired electrons and holes occupy their first single-carrier levels and an additional hole occupies the second single-hole energy level. The unpaired hole's spin projection along the growth axis determines the total spin of the two Kramers' degenerate states [for simplicity only one state is drawn in Fig. 1(a)]. Radiative recombination of first-level electron-hole (e-h) pair leaves three unpaired charge carriers within the QD. There are eight possible different spin configurations for the remaining carriers. These configurations form four energy levels of Kramers' pairs, depending on the relative spin orientations of the charge carriers.[26,27] The lowest three levels are those in which the two unpaired holes are in spin-triplet states. Those states are separated from the highest energy level in which the holes are in a singlet spin state by the hole-hole isotropic exchange interaction, which is significantly stronger than the e-h exchange interaction. The later removes the degeneracy between the triplet states as shown in Fig. 1(a). The lowest triplet level, in which the three carriers have parallel spins, cannot be reached optically. The optical transitions into the two other triplet levels, as well as to the singlet level, are optically allowed, as shown in the figure. The circular polarizations of the emitted photons are also given in the figure. They depend on the spins of the annihilated electron-hole pair.

In reality, however, one measures elliptical polarizations, which contain linear components [see Fig. 1(c)], due to the anisotropic e-h exchange interaction.[26,27] Hole-hole anisotropic exchange interaction[28] is not included in the analysis presented here, since the observed line multiplicities, energetic order, intensity ratios, and degrees of linear polarization are very well described without it (see Fig. 1).

From the intermediate states the relaxation proceeds by radiative recombination of the remaining first-level e-h pair, leaving thus only one hole in its second level. The hole can then quickly relax nonradiatively to its ground level. There is a fundamental difference between the singlet and triplet in-

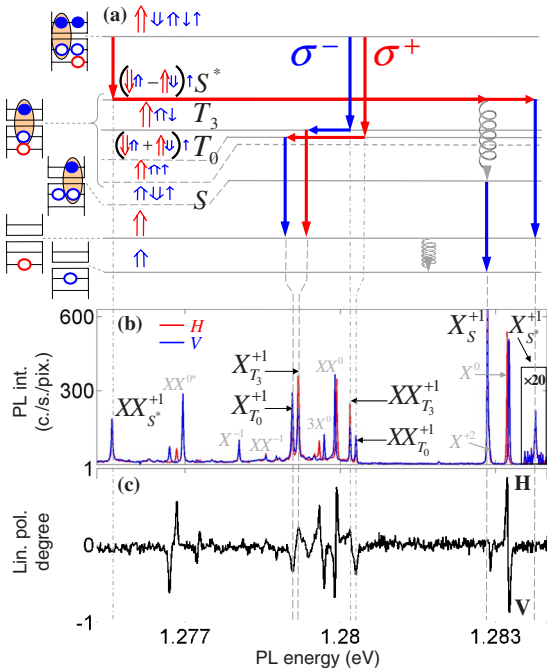

FIG. 1. (Color online) (a) Schematic description of the energy levels of a singly positively charged QD. Vertical (curly) arrows indicate radiative (nonradiative) transitions between these levels. State occupation and spin wave functions are described to the left of each level where $\uparrow(\Downarrow)$ represents an electron (hole) with spin up (down). A short blue (dark gray) [long red (light gray)] arrow represents a carrier in its first (second) level. $S(T)$ stands for two holes' singlet (triplet) state and 0 (3) for $S_z=0(S_z=\pm 3)$ total holes' spin projection on the QD growth direction. Only one out of two (Kramers') degenerate states is described. (b) Measured polarized PL spectra on which the actual transitions are identified. Red (blue) line represents the spectrum polarized along the major (H) [minor (V)] axis of the QD. Excitonic (biexcitonic) transitions are marked by dash (dash-dot) lines. Transitions which are not discussed here are marked by gray letters. (c) Measured degree of linear polarization spectrum, along the in-plane symmetry axes of the QD. Positive (negative) value represents polarization along the $H(V)$ direction.

termediate states. While in the later, due to Pauli's exclusion principle, radiative recombination, or spin scattering must occur before the excited hole can relax to its ground state (resulting in two "direct" cascades), in the former, nonradiative spin-preserving relaxation of the excited hole may occur prior to the radiative recombination (resulting in one direct and one "indirect" cascade). These four different possible radiative cascades are schematically described in Fig. 1(a). Their first experimental observation is described below.

The sample that we study was grown by molecular-beam epitaxy on a (001) -oriented GaAs substrate. One layer of strain-induced InGaAs QDs was deposited in the center of a 285-nm-thick intrinsic GaAs layer. The layer was placed between two distributed Bragg reflecting mirrors, made of 25 (bottom) and 10 (top) periods of pairs of AlAs/GaAs quarter wavelength thick layers. This constitutes a one optical wavelength (in matter) microcavity for light emitted due to recombination of QD confined e-h pairs in their lowest energy levels.

For the optical measurements the sample was placed inside a tube immersed in liquid helium, maintaining sample temperature of 4.2 K. A ×60, 0.85 numerical aperture, *in situ* microscope objective was used both to focus the exciting beam on the sample surface and to collect the emitted light. The collected light was split by a nonpolarizing beam splitter, and each beam was dispersed by a 1 m monochromator and detected by either an electrically cooled charge-coupled-device array detector or by a single channel, single photon, silicon avalanche photodetector, providing spectral resolution of about 10 μeV. The polarization of the emitted light in each beam was analyzed using two computer controlled liquid crystal variable retarders and a linear polarizer. The retarders were carefully calibrated at the emission wavelength such that cross talks between various polarization projections never exceeded 5%. Standard photon counting electronics was then used to measure the differences between the arrival times of two photons originating from two different spectral lines, at given polarizations. The response function of the system and its temporal resolution (~300 ps) were determined by measuring picosecond laser pulses.[17,20]

In Fig. 1(b) we present two polarization sensitive photoluminescence (PL) spectra measured under nonresonant cw excitation with 1 μW of HeNe laser light (1.96 eV). The spectral degree of linear polarization is presented in Fig. 1(c). The spectral lines observed were identified by various means such as excitation intensity-dependent PL, polarization memory measurements, and detailed comparison with a many carriers theoretical model.[29,30] The various lines are conventionally marked on Fig. 1(b).[29] The biexcitonic (excitonic) transitions participating in the radiative cascades described in Fig. 1(a) are marked by dash-dot (dash) lines.

The three direct and one indirect radiative cascades are clearly identified spectrally in the single QD PL [Fig. 1(b)] and linear polarization spectra [Fig. 1(c)]. Overall the measured spectrum and its polarization agree well with the calculated one,[29] but, in particular, few simple observations can be readily understood without relating to the detailed model: (a) all the positively charged lines are enhanced together (not shown) upon preferred positive charging of the QD using different excitation sources. (b) The biexciton lines and exciton lines have typical excitation intensity dependence. We note, in particular, that the intensity ratio between the neutral exciton and neutral biexciton is similar to that of the positively charged ones. (c) The energy sum of the two photons in each one of the three direct cascades is exactly the same. (d) The intensity ratio between the T_3 and T_0 biexcitonic and excitonic transitions is roughly 2:1 as readily expected from their spin-wave functions. (e) The T_3 excitonic and biexcitonic lines are linearly polarized horizontally (~20%) while the T_0 excitonic and biexcitonic lines are linearly polarized vertically (~40%) due to the anisotropic e-h exchange-induced mixing between the two intermediate levels. The direction of the linear polarizations and their ratio are in perfect agreement with the theory, though the absolute values are somewhat smaller than the calculated ones.[27,29]

In Fig. 2 we present the measured intensity correlation functions for photon pairs emitted in the four spin-conserving cascades outlined in Fig. 1(a). Radiative cascades are readily identified by the enhancement in the number of coincidences within one radiative lifetime from the detection

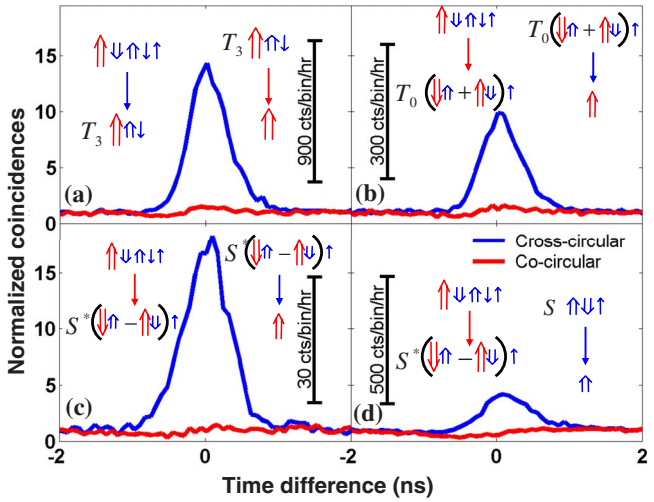

FIG. 2. (Color online) Measured time-resolved, polarization sensitive intensity correlation functions, for the four radiative cascades described in Fig. 1. Zero time indicates the detection of the first photon, negative times indicate reverse order of detections. The direct cascades involving T_3, T_0, and S^* as intermediate levels are presented in (a)–(c), respectively. The indirect cascade in which S^* is the intermediate state after the first photon and the ground $X^{+1}(S)$ is the second emitting state presented in (d). The states involved in the first (second) photon emission are illustrated to the left (right) side of each panel. All symbols are as in Fig. 1. Blue (red) line stands for measured relative cross- (co-) circularly polarized photons. The bar presents the acquisition rate in coincidences per time bin (80 ps) per hour.

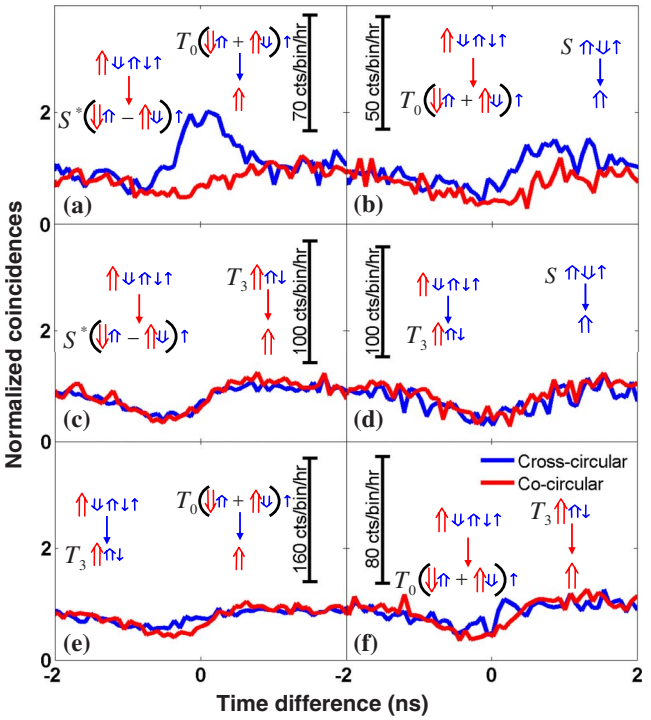

FIG. 3. (Color online) Measured time-resolved, polarization sensitive intensity correlation measurements, between the radiative cascades. (a) [(c)] Correlations between the S^* biexciton and the T_0, [T_3] exciton. (b) [(d)] Correlations between the T_0, [T_3] biexciton and the ground $X^{+1}(S)$ exciton. (e) [(f)] Correlation between the $T_3[T_0]$ biexciton and the $T_0[T_3]$ exciton. The meanings of all symbols are as in Fig. 2.

of the first photon.[17,20] Indeed, the measured data clearly reveal the temporal sequence of the radiative events. This, together with the enhanced signals at cross circular polarizations, reassure the spectral interpretations of Fig. 1. We note that while the cocircular coincidence signals [red (light gray) lines] involving the intermediate S^* level [Figs. 2(c) and 2(d)] are almost null, these involving the intermediate triplet states [Figs. 2(a) and 2(b)] are not. This indicates that while in the first case the photons are circularly polarized, in the second case they are slightly elliptically polarized due to the e-h anisotropic exchange mixing.[26,27,29] Therefore, following the detection of a circularly polarized biexciton photon, there are nonzero probabilities to find the system in either one of the two Kramers states of the relevant exciton level. These probabilities are given by the mixing degree induced by the anisotropic interaction. The mixing degree is obtained from the measured degree of linear polarization of the biexciton transitions. The probability for sequential emission of a circularly polarized exciton photon is now given by the sum of population probabilities of its Kramers states, weighted again by the same mixing degree.[27] As expected, we obtain the same mixing degree of $\sim 2.5\%$ for both biexciton lines.

In Fig. 3 we present intensity correlation measurements between different radiative cascades. These measurements provide means for estimating the degree of cross talk between the various optical cascades. Since spin blockading prevents the relaxation of the second level hole to its first level, they provide an estimate for the rate by which the hole spin's scatters.[30]

In Figs. 3(a) and 3(c) we probe possible transitions from the S^* singlet state to the triplet T_0 and T_3 intermediate states, respectively. In (b) and (d) we probe possible transitions from the triplet T_0 and T_3 intermediate states, respectively, to the singlet S ground state. Assuming that relaxation from the intermediate triplet states to the ground singlet state must be preceded by transition to the intermediate S^* singlet level, these measurements provide quantitative estimations for the reverse of the processes described in (a) and (c). In (e) and (f) we probe possible transitions between the T_3 and T_0 triplet intermediate states.

From the measured data in Fig. 3 one clearly notes that the nonradiative transitions which do not preserve the total holes' spin projection on the QD symmetry axis ($S^* \leftrightarrow T_3$ and $T_3 \leftrightarrow T_0$) are nearly forbidden on the radiative time scale [Figs. 3(c)–3(f)], whereas transitions which do preserve the total spin projection ($S^* \leftrightarrow T_0$) are partially allowed [Figs. 3(a) and 3(b)]. This means that the holes' spin projection on the QD's growth axis is conserved during the relaxation while their in-plane spin projection scatters.[30] The difference between the scattering rates from the singlet to triplet ($S^* \rightarrow T_0$) and that from the triplet to singlet ($T_0 \rightarrow S^*$) is due to the energy difference between these two states (~ 4 meV), which is larger than the ambient thermal energy (~ 0.5 meV).

The radiative rate ($\gamma_r = [0.8\ \text{ns}]^{-1}$) was directly measured from the temporal decay of the PL intensity of the excitons

(not shown). The $S^* \rightarrow S$ rate ($\Gamma_{S^* \rightarrow S} = 35\gamma_r$) was then deduced from the ratio between the integrated intensity of the PL emission from the S^* spectral line and that from the X^{+1} line. With these rates at hand we deduced the various spin-scattering rates from the total number of coincidences in Fig. 3. The rates for hole spin scattering which do not preserve the total spin projection on the QD growth direction was found to be much slower than the radiative rate ($\Gamma_{S^* \leftrightarrow T_3} \sim \Gamma_{T_0 \leftrightarrow T_3} \sim 0$). The relaxation rate which do preserve the total two-hole spin projection along the growth direction [$\Gamma_{S^* \rightarrow T_0} = 10\gamma_r$, deduced directly from Fig. 3(a)] is about an order of magnitude faster than the radiative rate, while the opposite rate [$\Gamma_{T_0 \rightarrow S^*} = 0.6\gamma_r$, deduced from Fig. 3(b)] is comparable to it. The ratio between these rates is an estimate for the temperature of the optically excited QD ($\sim$19 K).

The rates $\Gamma_{S^* \leftrightarrow T_3}$ and $\Gamma_{S^* \leftrightarrow T_0}$ are governed by single-hole's longitudinal (T_1^{-1}) and transverse (T_2^{-1}) spin-scattering rates, mainly of the decaying *p*-shell hole.[30] The first transition requires complete reversal of the *p*-shell hole's spin, from parallel to antiparallel to the spin state of the *s*-shell hole. The second transition involves transverse spin scattering, resulting in relative phase reversal between the spins of the two holes.

In summary, we identified three direct and one indirect radiative cascades in singly charged QDs, and demonstrated unambiguous correlations between the polarizations of the emitted photons and the spin of the remaining charge carrier. Our correlation measurements show that while single-hole spin lifetimes are much longer than the radiative time, their transverse spin-scattering times are almost an order of magnitude shorter. Our novel observations are useful for correlating anchored spin qubits with flying photon polarization qubits.

The support of the U.S.-Israel Binational Science Foundation (BSF), the Israeli Science Foundation (ISF), the Ministry of Science and Technology (MOST) and that of the Technion's RBNI are gratefully acknowledged.

*poem@technion.ac.il

[1] S. J. Freedman and J. F. Clauser, Phys. Rev. Lett. **28**, 938 (1972).
[2] A. Aspect, J. Dalibard, and G. Roger, Phys. Rev. Lett. **49**, 1804 (1982).
[3] Phys. World **11**(3) (1998), special issue on quantum information.
[4] A. Ekert and R. Jozsa, Rev. Mod. Phys. **68**, 733 (1996).
[5] A. Zeilinger, Rev. Mod. Phys. **71**, S288 (1999).
[6] C. Monroe, D. M. Meekhof, B. E. King, W. M. Itano, and D. J. Wineland, Phys. Rev. Lett. **75**, 4714 (1995).
[7] D. Loss and D. P. DiVincenzo, Phys. Rev. A **57**, 120 (1998).
[8] J. R. Petta, A. C. Johnson, J. M. Taylor, E. A. Laird, A. Yacoby, M. D. Lukin, C. M. Marcus, M. P. Hanson, and A. C. Gossard, Science **309**, 2180 (2005).
[9] D. Press, T. D. Ladd, B. Zhang, and Y. Yamamoto, Nature (London) **456**, 218 (2008).
[10] A. J. Ramsay, S. J. Boyle, R. S. Kolodka, J. B. B. Oliveira, J. Skiba-Szymanska, H. Y. Liu, M. Hopkinson, A. M. Fox, and M. S. Skolnick, Phys. Rev. Lett. **100**, 197401 (2008).
[11] P. Michler, A. Kiraz, C. Becher, W. V. Schoenfeld, P. M. Petroff, L. Zhang, E. Hu, and A. Imamoğlu, Science **290**, 2282 (2000).
[12] O. Benson, C. Santori, M. Pelton, and Y. Yamamoto, Phys. Rev. Lett. **84**, 2513 (2000).
[13] Z. Yuan, B. E. Kardyna, R. M. Stevenson, A. J. Shields, C. J. Lobo, K. Cooper, N. S. Beattie, D. A. Ritchie, and M. Pepper, Science **295**, 102 (2002).
[14] C. Santori, D. Fattal, J. Vučković, G. S. Solomon, and Y. Yamamoto, Nature (London) **419**, 594 (2002).
[15] D. Fattal, K. Inoue, J. Vučković, C. Santori, G. S. Solomon, and Y. Yamamoto, Phys. Rev. Lett. **92**, 037903 (2004).
[16] E. Moreau, I. Robert, L. Manin, V. Thierry-Mieg, J. M. Gérard, and I. Abram, Phys. Rev. Lett. **87**, 183601 (2001).
[17] D. V. Regelman, U. Mizrahi, D. Gershoni, E. Ehrenfreund, W. V. Schoenfeld, and P. M. Petroff, Phys. Rev. Lett. **87**, 257401 (2001).
[18] A. Kiraz, S. Falth, C. Becher, B. Gayral, W. V. Schoenfeld, P. M. Petroff, L. Zhang, E. Hu, and A. Imamoglu, Phys. Rev. B **65**, 161303(R) (2002).
[19] C. Santori, D. Fattal, M. Pelton, G. S. Solomon, and Y. Yamamoto, Phys. Rev. B **66**, 045308 (2002).
[20] N. Akopian, N. H. Lindner, E. Poem, Y. Berlatzky, J. Avron, D. Gershoni, B. D. Gerardot, and P. M. Petroff, Phys. Rev. Lett. **96**, 130501 (2006).
[21] R. Hafenbrak, S. M. Ulrich, P. Michler, L. Wang, A. Rastelli, and O. G. Schmidt, New J. Phys. **9**, 315 (2007).
[22] D. Gammon, E. S. Snow, B. V. Shanabrook, D. S. Katzer, and D. Park, Phys. Rev. Lett. **76**, 3005 (1996).
[23] V. D. Kulakovskii, G. Bacher, R. Weigand, T. Kümmell, A. Forchel, E. Borovitskaya, K. Leonardi, and D. Hommel, Phys. Rev. Lett. **82**, 1780 (1999).
[24] F. Troiani and C. Tejedor, Phys. Rev. B **78**, 155305 (2008).
[25] J. E. Avron, G. Bisker, D. Gershoni, N. H. Lindner, E. A. Meirom, and R. J. Warburton, Phys. Rev. Lett. **100**, 120501 (2008).
[26] K. V. Kavokin, Phys. Status Solidi A **195**, 592 (2003).
[27] I. A. Akimov, K. V. Kavokin, A. Hundt, and F. Henneberger, Phys. Rev. B **71**, 075326 (2005).
[28] T. Warming, E. Siebert, A. Schliwa, E. Stock, R. Zimmermann, and D. Bimberg, Phys. Rev. B **79**, 125316 (2009).
[29] E. Poem, J. Shemesh, I. Marderfeld, D. Galushko, N. Akopian, D. Gershoni, B. D. Gerardot, A. Badolato, and P. M. Petroff, Phys. Rev. B **76**, 235304 (2007).
[30] E. Poem, S. Khatsevich, Y. Benny, I. Marderfeld, A. Badolato, P. M. Petroff, and D. Gershoni, Solid State Commun. **149**, 1493 (2009).